MEISAM NASROLLAHI, Ph.D. Candidate[1]
E-mail: m_nasrollahi@ut.ac.ir
JAFAR RAZMI, Prof.[1]
E-mail: jrazmi@ut.ac.ir
REZA GHODSI, Prof.[1]
(Corresponding author)
E-mail: ghodsi@ut.ac.ir
[1] School of Industrial Engineering
College of Engineering, University of Tehran
Kargar Shomali St, Tehran, Iran

Traffic and Environment (Ecology)
Original Scientific Paper
Submitted: 21 Oct. 2017
Accepted: 10 July 2018

A COMPUTATIONAL METHOD FOR MEASURING TRANSPORT RELATED CARBON EMISSIONS IN A HEALTHCARE SUPPLY NETWORK UNDER MIXED UNCERTAINTY: AN EMPIRICAL STUDY

ABSTRACT

Measuring carbon emissions is an essential step in taking required action to fight global warming. This research presents a computational method for measuring transport related carbon emissions in a healthcare supply network. The network configuration significantly impacts carbon emissions. First, a multi-objective mathematical programming model is developed for designing a healthcare supply network in the form of a two-graph location routing problem under demand and fuel consumption uncertainty. Objective functions are minimizing total cost and minimizing total fuel consumption. In the presented model, the demand of each customer must be completely satisfied in each time period, and backlog is not permitted. The number and capacity of vehicles are determined, and vehicles are heterogeneous. Furthermore, fuel consumption depends on traveling distance, vehicle and road conditions, and the load of a vehicle. The centroid method is applied to face demand uncertainty. Next, a multi-objective non-dominated ranked genetic algorithm (M-NRGA) is proposed to solve the model. Then, a Monte Carlo based approach is presented for measuring transport-related carbon emissions based on fuel consumption in supply network. Finally, the proposed approach is applied to the case of a healthcare supply network in the Fars province in Iran. The obtained results illustrate that the proposed approach is a practical tool in designing healthcare supply networks and measuring transport-related carbon emissions in the network.

KEY WORDS

healthcare; greenhouse effect; supply network; carbon emissions; Monte Carlo;

1. INTRODUCTION

Environmental changes and global warming are among the most important challenges humans have faced in the last hundred years [1, 2]. Earth system simulation shows that the current trend of greenhouse gas emissions may affect most ecosystems and the lives of over 3.5 billion people worldwide as early as 2050 [3]. Carbon dioxide (CO_2) and carbon monoxide (CO) are the primary greenhouse gases emitted through human activities. As the most important cause of long-term climate change, carbon emissions provide a good baseline to assess progress and evaluate the consequences. The current emission trends continue to follow scenarios that lead to the highest global temperature increases [4]. Carbon emissions produced by human activities usually come from burning fossil fuels, e.g. oil, natural gas, coal, and wood [5].

To overcome this challenge, governments and industry sectors are working to understand their own carbon footprint and explore the required actions. Reducing the global temperature and associated climate change impacts can be achieved by decreasing the emissions of greenhouse gases as soon as possible [6]. The experiences of the largest global corporations as well as those of start-up companies indicate how these companies can profitably reduce greenhouse gas emissions in their supply chains [7]. Approximately 45% of greenhouse gas emissions is caused by production and transportation of goods [8]. Hence, it is important to restrict such emissions in a supply network.

In the past decades, many researchers have focused on modeling the uncertainty in designing supply networks. For this aim, different stochastic modeling approaches have been successfully applied to supply chain production planning problems considering the randomness concept. However, in some applications, the probability distributions are not available or reliable [9]. On the other hand, in some real applications, the nature of retailer's demand is imprecise. In this case, fuzzy set theory (FST) provides a proper

framework for handling uncertainty or vagueness in a dataset. In decision sciences, fuzzy set theory has a great impact on preference modeling and multi-criteria assessment by taking into account the user needs in optimization techniques [10]. Hence, in the proposed method, trapezoidal fuzzy numbers are used to characterize the fuzzy demand for products, vehicle performance, and road conditions. Note that in most real applications of a supply chain problem there is not enough historical data for the previous demand values. In these cases, using fuzzy numbers can be used to describe the decision models for the external demand of a network. Although there is no conclusive methodology for measuring carbon emissions at present [11, 12], this research provides a computational method for measuring transport related carbon emissions (TRCE) in a supply network. First, a mathematical model to design proper supply network is developed, and then a computational method is proposed for measuring TRCE in this network, based on the Monte Carlo approach. In Section 2, a literature overview of supply network design and measuring carbon emissions is given. The mathematical model to design the supply network is presented in Section 3, followed by the solution approach and TRCE measuring approach. The case study, i.e., Fars healthcare supply network, is presented in Section 5. At the end, the conclusion and future study considerations finalize the paper.

2. LITERATURE REVIEW

Generally, the causes of carbon emissions can be divided into natural and human sources. The main carbon emissions due to human activities includes industries like cement and electricity production, commercial and residential causes, deforestation, agriculture, and transportation. Also, the major carbon footprint applications in the UK can be categorized by seven areas, including national emissions inventories and trade, emission drivers, economic sectors, supply chains, organizations, household consumption and lifestyles, as well as sub-national emission inventories. Researchers in [8, 13] state that to restrict the emissions of greenhouse gases, companies should take into account their business practices and operational policies along with focusing on their physical processes (inefficient equipment and facilities, redesigning products and packaging, finding less polluting sources of energy, or instituting energy saving programs). They attempted to explore how operational decisions across the supply chain affect the carbon footprint of these supply chains and the extent to which concerns about carbon emissions are covered by adjusting operational decisions and improving collaboration among supply chain partners. They also showed how carbon emission concerns can be integrated into operational decision-making with regard to procurement, production, and inventory management using relatively simple and widely used models.

The transportation of goods accounts for a large amount of carbon releasing all over the world. TRCE cannot be measured easily because of the large amount of data required and the use of different standards for carbon footprint calculation [14]. Several researchers proposed various methods for computing carbon emissions in a supply chain [15-20]. For instance, they calculated the carbon footprint of different feedstock for dairy cattle by applying life cycle assessment (LCA) [18]. Others proposed a fast and vigorous technique applying a novel approach based upon multi-gene genetic programming (MGGP) to determine carbon dioxide minimum miscibility pressure (CO_2 MMP) for carbon dioxide injection processes [19]. In [20], a "corrected average emission model" was provided, i.e., an improved average speed model that accurately computed CO_2 emissions on the road.

Transportation consumes energy severely worldwide and is overwhelmingly oil-oriented. For this reason, TRCE is one of the main sources of global carbon emissions and also contributes to air quality concerns, particularly in and around major population centers [21]. In this regard, [22] showed that most of the imported oil in the USA is consumed only in the transportation sector. Additionally, one third of total greenhouse gas (GHG) emissions is produced by this sector. For reducing GHG emissions and oil consumption, different policy scenarios must be considered in the US transportation sector. Therefore, proper green transportation network design is a suitable solution for decreasing carbon emission [23], [24].

Recently, in the period of global competition, the network design has been considered as one of the strategic decision problems. A network design problem focuses on the number and locations of raw material suppliers, manufacturing plants, and inventory warehouses. In an extended time horizon, the decisions in this regard include selecting the distribution channel from suppliers to customers as well as determining the transportation volume among distributed facilities [25]. The supply network design problem is well documented in the literature, and the readers are referred to the review the paper [26].

The vehicle routing problem (VRP) is the problem of designing routes for delivery vehicles with known capacities operating from a single depot to supply a number of customers with known locations and known demands for a certain commodity. Vehicle routes are designed to minimize several objectives, like the total distance traveled [27]. For instance, the authors in [28] presented a new mathematical model in order to measure and evaluate the efficiency of the periodic vehicle routing problem (PVRP) in a competitive environment. A general model for dynamic vehicle routing

problem with time windows (DVRPTW) considering the minimization of the total distance as the main objective was presented in [29]. A review paper highlighted major exact algorithms in the VRP literature [30]. They focused on mathematical formulations, relaxations, and recent exact methods for two main VRP variants, including the capacitated VRP (CVRP) and the VRP with time windows (VRPTW). For detailed information about VRP, please refer to the review paper [30].

As one type of the network design problem, the location routing problem (LRP) deals with the combination of both the facility location problem (FLP) and the vehicle routing problem (VRP). Since these two categories of problems belong to the class of NP-hard problems, the LRP is also an NP-hard problem. In the LRP, the entire consumer demand should be satisfied in such a way that a facility's operating and fixed costs are minimized while vehicle capacities must be considered and routing costs must be reduced simultaneously [31]. Several researchers have developed heuristic and meta-heuristic algorithms for LRP [32-34]. A new heuristic algorithm for the capacitated location routing problem (CLRP) was presented in [35], called granular variable tabu neighborhood search (GVTNS). In order to solve the periodic location routing problem (PLRP), a large neighborhood search (LNS) algorithm was presented in [36].

Recently, researchers and practitioners have taken into account the environmental concerns in designing supply networks. In this respect, decisions on supply chain design have to be integrated with those related to environmental concerns. In other words, a green supply chain network design problem contains an initial investment into environmental protection equipment or techniques to ensure its long-term benefit to environmental indicators [37]. Fortunately, due to the importance of the green supply chain concept, a lot of research has been focused on this area. Please see the comprehensive survey provided by [38] for more detailed information. Most research on designing a green supply network has considered a deterministic behavior for the supply network. However, in most practical situations, we may face numerous sources of technical and/or commercial uncertainty in the design phase.

The concept of uncertainty in LRP problems is considered in several studies [33], [39-43]. The authors in [44] described the impact of network type on uncertainty in demand estimation. They suggested that the configuration of the network can affect the final accumulation of uncertainty in the supply chain. The authors in [45] identified the impact of the accumulation of individual delivery time uncertainties on overall delivery time uncertainty. Also, they stated that the type of network and their structures have a significant influence on delivery time uncertainty. In order to prove their idea, they created a probabilistic technique for measuring and evaluating that impact by using the Markov theorem.

In this paper, we simultaneously take into account the environmental concerns and uncertainty conditions in a healthcare supply network. A multi-objective non-dominated ranked genetic algorithm (M-NRGA) is proposed to solve the developed multi-objective mathematical model. A Monte Carlo based approach is presented to measure transport-related carbon emissions based on fuel consumption in a supply network. We also represent the application of the proposed approach to the case of the healthcare supply network in the Fars province in Iran.

3. PROBLEM DEFINITION

3.1 Healthcare supply network

In the presented healthcare supply network, a number of distribution centers should be located among candidate sites. Furthermore, delivery routes between the central depot and these distribution centers as well as delivery routes for a set of customers must be established in such a way that the total system cost is minimized. Therefore, the network configuration includes a two-graph location routing problem. In one graph, a fleet of vehicles with known capacities is operating from a central depot to supply a number of distribution centers which should be located among candidate sites. All vehicle routes start and end at the central depot. The demand of each distribution center must be completely satisfied, and backlog is not permitted. All distribution centers are visited exactly once by exactly one vehicle in each time period, so split delivery is not permitted. The sum of distribution centers' demand for any vehicle route may not exceed vehicle capacity. In the other graph, the network configuration is a multi-depot vehicle routing problem in which a fleet of vehicles with known capacities operate from a central depot to supply a number of customers with known locations. Each vehicle route starts and ends at the same distribution center. The demand of each customer must be completely satisfied, and backlog is not permitted. All customers are visited exactly once by exactly one vehicle in each time period, so split delivery is not permitted; the sum of customers' demand for any vehicle route may not exceed the vehicle capacity. A direct delivery from the central depot to the customers is not permitted, as well as a delivery from one distribution center to the other. In summary, we face a two-graph location routing problem, i.e., to simultaneously determine the number and locations of distribution centers, assignment of customers to distribution centers, and vehicle routes. *Figure 1* illustrates the healthcare supply network. In the proposed model, there are multiple time periods in the planning

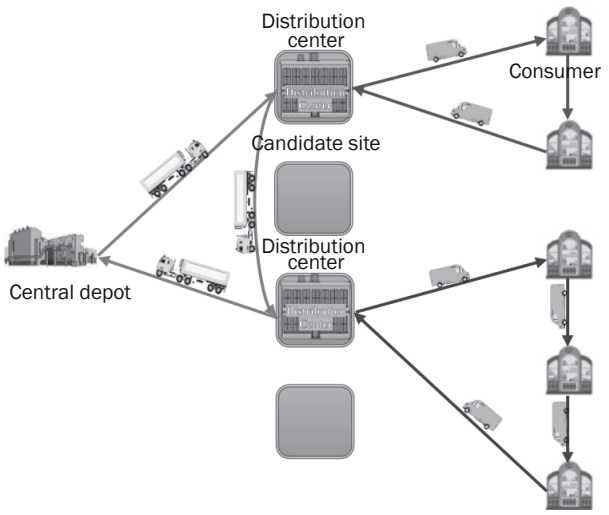

Figure 1 – Healthcare supply network

horizon. The customers' demand for each product is a trapezoidal fuzzy number ($\tilde{d}=(d_1,d_2,d_3,d_4)$ where: $d_1 \leq d_2 \leq d_3 \leq d_4$) on $\mathbb{R}$). The membership function of the trapezoidal fuzzy number is presented in *Equation 1* [46].

$$\mu_{\tilde{d}}(x)=\begin{cases}\frac{x-d_1}{d_2-d_1} & d_1<x<d_2\\ 1 & d_2<x<d_3\\ \frac{d_4-x}{d_4-d_3} & d_3<x<d_4\\ 0 & Otherwise\end{cases} \quad (1)$$

In *Equation 1*, if $d_2=d_3$, then $\tilde{t}$ is a triangular fuzzy number. Also, if $d_1=d_2=t_3=t_4$, then $\tilde{t}$ is a crisp number. *Figure 2* illustrates the membership function of the trapezoidal fuzzy number.

The number and capacity of vehicles and candidate locations for distribution centers are determined. Vehicles are heterogeneous and can take only one tour in each time period. The objectives are minimizing the total cost of the system and minimizing total fuel consumption. Fuel consumption depends on traveling distance, vehicle and road conditions, and the load of a vehicle. All of these quotients are trapezoidal fuzzy numbers.

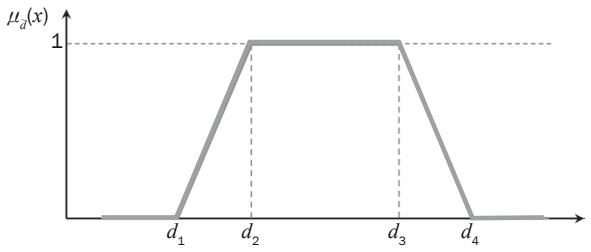

Figure 2 – Membership function of the trapezoidal fuzzy number

Assumptions

- The selection of the central depot and customers' location is beyond the scope of this paper, but the locations of distribution centers are determined by the presented model
- The vehicles are heterogeneous
- Split delivery is not permitted
- The capacities of distribution centers and vehicles are definite
- The routing process is performed between customer – distribution center echelons and central depot – distribution center echelons. Hence, the VRP is a multi-graph problem.
- It is not possible to stock pharmaceutical substances for future periods in distribution centers
- Demand is considered to be uncertain
- Fuel consumption per distance unit is considered to be uncertain
- Fuel consumption per load unit is considered to be uncertain
- Time windows for distribution centers and customers are not considered.

3.2 Mathematical model for healthcare supply network design

The proposed mathematical programing formulation is presented below:

Sets:

I - Set of customers indexed by i=1,2,...,N; where N is the number of customers

J - Set of candidate locations indexed by j=0,1,2,...,P; where P is the number of candidate locations. 0 is the central depots index

G - Set of all supply network graph nodes $G=I\cup J=\{0,1,2,...,P,P+1,...,P+N\}$

A - Set of arcs (i,j)

T - Set of time periods indexed by t=1,2,...,K; where K is the number of time periods in the planning horizon

M - Set of products indexed by m=1,2,...,M; where M is the number of products distributed in the supply network

V - Set of vehicles indexed by v=1,2,...,V; where V is the number of available vehicles

Parameters:

$\tilde{d}_{im}^{t}$ - Customer i demand for product m in the period t

ξ_j - Fixed cost for opening a distribution center in the candidate location j

ζ_v - Fixed cost for using vehicle v

γ_{ij} - The distance along the arc $(i,j)\in A$

ϖ_{ij}^{v} - Traveling cost per distance unit for vehicle v in arc $(i,j)\in A$

α_j^m - The capacity of distribution center placed in node j for the product m. Capacity of central depot (α_0^m) is infinitive for all products.

β_v^m - Capacity v-th vehicle for product m
ϑ_m - Weight of each unit of product m
$\tilde{\omega}_0^v$ - Fuel consumption per distance unit for unloaded vehicle v in a road without slope
$\tilde{\omega}_1^v$ - Additional fuel consumption per distance unit for vehicle v associated with load unit
$\tilde{\omega}_2^v$ - Quotient of fuel consumption per distance unit for vehicle v associated with vehicle conditions
$\tilde{\omega}_3^{ijv}$ - Quotient of fuel consumption per distance unit for vehicle v associated with road conditions (arc $(i,j)\in A$)

Decision variables:
X_{ij}^{vt} - 1 if vehicle v at time period t travels in arc $(i,j)\in A$, and 0 otherwise
Y_{ij}^t - 1 if in time period t the demand of customer i is satisfied by the distribution center placed in node j, and 0 otherwise
Z_j - 1 if a distribution center open at candidate location j, and 0 otherwise
$\tilde{L}_{ij}^{vt}$ - Load of vehicle v traveling arc $(i,j)\in A$ at time period t
U_{iv}^t - Auxiliary variable for sub-tour elimination constraints in vehicle v route
U'^t_{iv} - Auxiliary variable for sub-tour elimination constraints in vehicle v route

Objective functions:

$$\min Z_1 = \sum_{\forall j} \xi_j Z_j + \sum_{j\in J}\sum_{v\in V}\sum_{t\in T} \zeta_v X_{0j}^{vt} + \sum_{i\in I}\sum_{\substack{j\in J\\ j\neq 0}}\sum_{v\in V}\sum_{t\in T} \zeta_v X_{ij}^{vt} + \sum_{i\in G}\sum_{j\in G}\sum_{v\in V}\sum_{t\in T} \varpi_{ij}^v \gamma_{ij} X_{ij}^{vt} \quad (2)$$

$$\min Z_2 = \sum_{i\in G}\sum_{j\in G}\sum_{v\in V}\sum_{t\in T} \left(\tilde{\omega}_0^v + \tilde{\omega}_1^v \tilde{L}_{ij}^{vt} + \tilde{\omega}_2^v + \tilde{\omega}_3^{ijv}\right)\gamma_{ij} X_{ij}^{vt} \quad (3)$$

Subject to:

$$\sum_{i\in I} \tilde{d}_{im}^t Y_{ij}^t \le a_j^m Z_j \quad \forall j\in J;\forall m\in M;\forall t\in T \quad (4)$$

$$\tilde{d}_{jm}^t = \sum_{i\in I} \tilde{d}_{im}^t Y_{ij}^t \quad \forall j\in J;\forall m\in M;\forall t\in T \quad (5)$$

$$\sum_{i\in G}\sum_{j\in G} \tilde{d}_{im}^t X_{ij}^{vt} \le \beta_v^m \quad \forall m\in M;\forall v\in V;\forall t\in T \quad (6)$$

$$\sum_{\substack{i\in G\\ j\neq 0}}\sum_{v\in V} X_{ij}^{vt} \le 1 \quad \forall i\in I;\forall t\in T \quad (7)$$

$$\sum_{\substack{i\in G\\ i\notin i}}\sum_{v\in V} X_{ij}^{vt} \le 1 \quad \forall j\in J;\forall t\in T \quad (8)$$

$$\sum_{i\in G}\sum_{j\in G} X_{ij}^{vt} \le 1 \quad \forall v\in V;\forall t\in T \quad (9)$$

$$\tilde{L}_{0j}^{vt} = \sum_{i}\sum_{\substack{j\\ j\neq 0}}\sum_{m\in M} \tilde{d}_{jm}^t \vartheta_m X_{0j}^{vt} \quad \forall v\in V;\forall t\in T \quad (10)$$

$$\tilde{L}_{ji}^{vt} = \sum_{i}\sum_{j,j\neq 0}\sum_{m\in M} \tilde{d}_{im}^t \vartheta_m X_{ij}^{vt} \quad \forall v\in V;\forall t\in T \quad (11)$$

$$\sum_{j\in G} X_{ij}^{vt}\tilde{L}_{ij}^{vt} - \sum_{j\in G} X_{ji}^{vt}\tilde{L}_{ji}^{vt} = \sum_{j\in G} X_{ij}^{vt}\tilde{d}_{jm}^t\vartheta_m \quad \forall i\in G;\forall v\in V;\forall t\in T \quad (12)$$

$$U_{lv}^t - U_{iv}^t + NX_{li}^{vt} \le N-1 \quad \forall l\in I;\forall i\in I;\forall v\in V;\forall t\in T \quad (13)$$

$$U'^t_{kv} - U'^t_{jv} + NX_{kj}^{vt} \le P-1 \quad \forall k\in J;j\in J\&\neq 0;\forall v\in V;\forall t\in T \quad (14)$$

$$\sum_{j\in G} X_{ij}^{vt} - \sum_{j\in G} X_{ji}^{vt} = 0 \quad \forall i\in G;\forall v\in V;\forall t\in T \quad (15)$$

$$\sum_{k\in I} X_{jk}^{vt} + \sum_{k\in I} X_{ki}^{vt} \le Y_{ij}^t + 1 \quad (16)$$

$$X_{ij}^{vt}\in\{0,1\} \quad (17)$$

$$Y_{ij}^t\in\{0,1\} \quad (18)$$

$$Z_j\in\{0,1\} \quad (19)$$

$$\tilde{L}_{ij}^{vt}\ge 0 \quad (20)$$

$$U_{iv}^t\in\{N\cup 0\} \quad (21)$$

$$U_{iv}^t\in\{P\cup 0\} \quad (22)$$

Objective function 2 shows the sum of fixed costs of opening distribution centers in candidate locations, the sum of fixed costs for using vehicles at the central depot, the sum of fixed costs for using vehicles at distribution centers, and transportation costs. *Objective function 3* represents fuel consumption considering traveling distance, vehicle and road conditions, and the load of a vehicle.

Constraint 4 assures customers are allocated to distribution centers within their capacity. *Constraint 5* states that the demand of distribution center j is equal to sum of the demands of customers which are allocated to distribution center j. *Constraint 6* ensures that customers are visited within vehicle capacity. *Constraints 7* and *8* ensure that all customers and all distribution centers are visited once in each time period. *Constraint 9* states that each vehicle can take only one tour in each time period. *Constraints 10*, *11*, and *12* show the load of vehicles at each route. Sub-tour elimination in both graphs is assured in *Constraints 13* and *14*. The continuity of tours and returning the vehicle to the origin depot is ensured in *Constraint 15*. C*onstraint 16* states that customer can be allocated to a distribution center and distribution center can be allocated to central depot only if there is a route connected to them. The binary variables are defined in *Constraints 17*, *18,* and *19*. Finally, load and auxiliary variables taking positive values are declared in *Constraints 20*, *21*, and *22*.

4. SOLUTION APPROACH

The solution approach is presented in 3 steps. First, we present an approach for facing uncertainty; then we describe a method for solving the proposed optimization model for the network design problem; and, finally, we propose a Monte Carlo approach based approach for measuring TRCE.

In this paper, the centroid method is applied for the defuzzification of the trapezoidal fuzzy number. The centroid of the trapezoidal fuzzy number $\tilde{t}$ is shown in *Equation 23* [47].

$$C_{\tilde{t}} = \frac{t_3^2 + t_4^2 + t_3 t_4 - t_1^2 - t_2^2 - t_1 t_2}{3(t_3 + t_4 - t_1 - t_2)} \quad (23)$$

4.1 Solution algorithm

To solve the proposed model, we developed a two-phase algorithm based on non-dominated ranked genetic algorithm for solving multi-objective optimization problems (NRGA) and preference ranking organization method for enrichment of evaluations (PROMETHEE). In the first phase, the Pareto front is generated by NRGA; in the second phase, the best solution is determined by the PROMETHEE-II method.

NRGA was developed by Al Jadaan et al. [48]. In this paper, we develop a modified version of the multi-objective NRGA called M-NRGA. In NRGA, a two-phase selection method is implemented. In the first phase, one of the fronts is selected by a fitness proportionate selection procedure (roulette wheel) based on its rank, and in the next phase one chromosome is selected from this front. Therefore, in NRGA the possibility of selecting a chromosome depends on its front's rank [49]. In the proposed M-NRGA, to improve the quality of the solutions in the Pareto front, P_e percent of solutions are selected based on elitism from the elitist solutions in the first front. In addition, to increase the diversity of the solutions in the Pareto front, P_t percent of solutions are selected based on the tournament method. In the proposed M-NRGA, since P_e percent of solutions are selected based on elitism, it is possible to adjust the number of solutions in the Pareto front to be at least equal to a fixed number. The proposed M-NRGA, as described, is as follows:

1) Initialize the first generation of solutions randomly with the population size N.
2) Calculate both objective functions for all solutions.
3) Sort and locate the solution based on the method presented in [48].
4) Do the crossover operation for P_c and mutation for P_m presentation of population.
5) Select N solution for the next generation. Three strategies are applied to select the solutions:
   a) P_e percent of solutions are selected based on elitism from the elitist solutions in the first front.
   b) P_t percent of solutions are selected based on the tournament method. Two solutions are selected randomly. The one that belongs to the front with the higher rank wins. If the solutions come from the same front, the one with the higher rank in the front wins.
   c) P_r percent of solutions are selected based on the roulette wheel method. At first, the front is selected with the probability of P_F, as shown in *Equation 24*, and then the solution is selected with the probability of P_r from the selected front, as presented in *Equation 25*.

$$P_F = \frac{Rank_F}{\frac{NF}{2}(NF+1)} \quad (24)$$

$$P_r = \frac{Rank_{sF}}{\frac{NSF_F}{2}(NSF_F+1)} \quad (25)$$

where NF is the number of fronts, $Rank_F$ is the rank of front F, NSF_F is the number of solutions in front F, and $Rank_{sF}$ is the rank of solution s in front F.

6) If the end condition is satisfied, the solution approach is over, otherwise go back to step 3.

In the second phase, the best solution is identified by PROMETHEE-II from the best Pareto front obtained in the previous phase. The PROMETHEE was first developed by Brans and Vincke in 1985 [50]. PROMETHEE-I can provide a partial ranking, while PROMETHEE-II can drive total ranking of the solutions. Therefore, in this paper, we use PROMETHEE-II. The method we applied is exactly as it described in [51].

4.2 Measuring TRCE

Measuring TRCE based on fuel consumption is not a straightforward processs. The amount of carbon emission depends on many factors such as the quality of fuel, vehicle conditions, weather conditions, the load of vehicle, etc. Therefore, in the mathematical formulation based on fuel consumption for TRCE, the carbon emission quotient is a probabilistic parameter. Due to *Equation 3*, TRCE can be measured by *Equation 26*.

$$TRCE = \hat{\psi}\left[\sum_{i\in G}\sum_{j\in G}\sum_{v\in V}\sum_{t\in T}(\tilde{\omega}_0^v + \tilde{\omega}_1^v \tilde{L}_{ij}^{vt} + \tilde{\omega}_2^v + \tilde{\omega}_3^{ijv})\gamma_{ij} X_{ij}^{vt}\right] \quad (26)$$

where $\hat{\psi}$ is a probabilistic parameter probability density function $f(y)$ for the carbon emission quotient. The cumulative distribution function F_Y is defined as *Equation 27*.

$$F_Y = \int_{-\infty}^{y} f(y)\,dy \quad (27)$$

To calculate TRCE, we applied a Monte Carlo based approach. The suggested algorithm is as follows:

1) Estimate the probability density function for carbon emission quotient $(\hat{\psi})$.
2) Create a vector with B array for each probabilistic and fuzzy number in *Equation 26* considering their probability density function or fuzzy membership function.
3) Calculate TRCE vector by *Equation 28*.

$$\hat{\psi} \qquad \tilde{\omega}_0^v \quad \forall v \qquad \tilde{\omega}_1^v \quad \forall v \qquad \tilde{L}_3^{ijv} \quad \forall i,j \,\&\, v \qquad \tilde{\omega}_2^v \quad \forall v \qquad \tilde{\omega}_3^{ijv} \quad \forall i,j \,\&\, v$$

$$\begin{bmatrix}\psi_1\\ \psi_2\\ \vdots\\ \psi_B\end{bmatrix} \quad \begin{bmatrix}\omega_{0\,1}^v\\ \omega_{0\,2}^v\\ \vdots\\ \omega_{0\,B}^v\end{bmatrix} \quad \begin{bmatrix}\omega_{1\,1}^v\\ \omega_{1\,2}^v\\ \vdots\\ \omega_{1\,B}^v\end{bmatrix} \quad \begin{bmatrix}L_{3\ \ 1}^{ijv}\\ L_{3\ \ 2}^{ijv}\\ \vdots\\ L_{3\ \ B}^{ijv}\end{bmatrix} \quad \begin{bmatrix}\omega_{2\,1}^v\\ \omega_{2\,2}^v\\ \vdots\\ \omega_{2\,B}^v\end{bmatrix} \quad \begin{bmatrix}\omega_{3\ \ 1}^{ijv}\\ \omega_{3\ \ 2}^{ijv}\\ \vdots\\ \omega_{3\ \ B}^{ijv}\end{bmatrix}$$

Figure 3 – Vectors for probabilistic and fuzzy numbers

$$\begin{bmatrix}TRCE_1\\ TRCE_2\\ \vdots\\ TRCE_B\end{bmatrix} = \begin{bmatrix}\psi_1\\ \psi_2\\ \vdots\\ \psi_B\end{bmatrix} \cdot \left(\sum_{i\in G}\sum_{j\in G}\sum_{v\in V}\sum_{t\in T} \gamma_{ij} X_{ij}^{vt} \left(\begin{bmatrix}\omega_{01}^v\\ \omega_{02}^v\\ \vdots\\ \omega_{0B}^v\end{bmatrix} + \begin{bmatrix}\omega_{11}^v\\ \omega_{12}^v\\ \vdots\\ \omega_{1B}^v\end{bmatrix} \cdot \begin{bmatrix}L_{31}^{ijv}\\ L_{32}^{ijv}\\ \vdots\\ L_{3B}^{ijv}\end{bmatrix} + \begin{bmatrix}\omega_{21}^v\\ \omega_{22}^v\\ \vdots\\ \omega_{2B}^v\end{bmatrix} + \begin{bmatrix}\omega_{31}^{ijv}\\ \omega_{32}^{ijv}\\ \vdots\\ \omega_{3B}^{ijv}\end{bmatrix} \right) \right) \tag{28}$$

4) Calculate average and variance of resulted vector. That would present the average and variance of TRCE.
5) Draw the histogram of the transpose of resulted vector. From the sampling frequency of $[TRCE_1, TRCE_2, \ldots, TRCE_B]$, the probability density function of TRCE can be obtained.

5. CASE STUDY

5.1 Fars healthcare supply network

In this paper, Fars healthcare supply network is considered as the case study. Fars is one of the thirty-one provinces of Iran and located in the south of the country. Fars has one of the richest cultural heritages in Iran, encompassing many disciplines such as literature, poetry, architecture, and stonemasonry, and it is known as the cultural capital of Iran. In 2015, this province had a population of 4.6 million people [52]. Due to the capabilities of Fars healthcare industry, such as a remarkable number of hospitals, reputable physicians, high quality healthcare services, mild weather, tourist attractions, and good hotels, many patients from all over Iran, the Persian Gulf countries, and even Europe travel to Shiraz to receive healthcare services.

We consider five years as the planning horizon for the Fars healthcare supply network divided into 60 one-month periods. In the Fars healthcare supply network, as illustrated in *Figure 4*, the central depot is located in Shiraz. Shiraz is the capital city of the Fars province and the most populous city in the south of Iran with the population of 1.9 million [52]. There are 29 customers and 5 candidate locations for distribution centers in Shiraz, Fasa Eqlid, Firuzabad, and Lar. The distances between network nodes are given in *Table 1*. In this supply network, 2,447 types of products are distributed. The demand for each product is estimated based on recent 36-month demand. The total demand for all products in Fars is 2,405,281,094 annually. We used *Equation 23* to calculate the centroid of demands $(C_{\tilde{d}_{lm}^t})$. Some of the results are given in *Table 2*. Obviously, these 2,447 types of products increase the problem complexity unnecessarily. In order to simplify the problem, we classified the pharmaceutical substances into 47 major groups, as shown in *Table 3*.

Three different meta-heuristic algorithms, including NSGA-II, MOPSO, and the proposed M-NRGA, are used to solve the proposed optimization model for the network design problem. NSGA-II is one of the most popular multi-objective evolutionary algorithms,

Figure 4 – Fars healthcare supply network

Table 1 – Distances between network nodes

	Shiraz	Kazeroon	Marvdasht	Lar	Jahrom	Fasa	Darab	Firuzabad	Nourabad	Neyriz	Eqlid	Abadeh	Sepidan	Lamerd	Kavar	Hajiabad	Estahban	Qir	Kharameh	Mohr	Safashahr	Bavanat	Gerash	Rostam	Farashband	Arsenjan	Khonj	Sarvestan	Saadatshahr
Shiraz	0	160	39	378	192	130	225	93	158	192	267	265	100	464	60	250	160	169	84	509	187	230	359	180	164	135	286	83	119
Kazeroon	160	0	199	461	336	290	385	186	58	352	427	434	233	547	194	410	320	252	248	240	347	290	500	79	105	295	418	217	250
Marvdasht	39	199	0	417	242	169	267	132	197	231	228	235	139	503	107	408	199	208	83	548	148	191	413	223	177	96	332	130	66
Lar	378	461	417	0	201	284	379	285	519	392	645	625	478	224	294	628	361	252	330	269	565	608	23	507	356	513	113	289	450
Jahrom	192	336	242	201	0	83	178	160	351	190	460	499	293	356	145	203	160	77	197	401	380	423	185	358	231	328	169	156	101
Fasa	130	290	169	284	83	0	95	223	288	140	397	374	230	439	164	120	72	160	107	484	317	360	247	123	294	165	258	65	210
Darab	225	385	267	379	178	95	0	318	383	199	492	467	325	534	267	62	167	255	210	579	412	455	189	426	389	360	220	169	313
Firuzabad	93	186	132	285	160	223	318	0	234	385	360	367	193	371	59	342	253	76	194	416	280	223	245	283	71	228	169	163	226
Nourabad	158	58	197	519	351	288	383	234	0	350	425	432	175	605	216	224	318	210	271	295	345	288	522	17	305	293	441	240	272
Neyriz	219	352	231	392	190	140	199	385	350	0	459	466	292	546	231	289	32	367	122	591	379	422	286	390	356	327	317	133	207
Eqlid	265	427	228	645	460	397	492	360	425	459	0	130	367	731	267	517	427	426	243	776	107	460	573	240	421	210	491	283	157
Abadeh	274	434	235	625	499	374	467	367	432	466	130	0	404	728	330	524	87	442	245	783	434	467	597	288	438	274	555	285	158
Sepidan	100	233	139	478	293	230	325	193	175	293	367	404	0	564	162	250	260	269	178	609	287	293	468	135	264	235	387	185	196
Lamerd	464	547	503	224	356	439	534	371	605	546	731	728	564	0	324	714	516	295	459	45	651	694	146	515	442	599	133	427	490
Kavar	60	194	107	294	145	164	267	59	216	231	267	330	162	324	0	461	189	157	128	284	250	288	318	232	124	201	237	97	175
Hajiabad	250	410	408	628	203	120	62	342	224	289	517	524	250	741	461	0	192	280	404	759	437	408	283	620	414	385	373	363	482
Estahban	160	320	199	361	160	72	167	253	318	32	427	87	260	516	189	192	0	237	106	561	347	160	314	348	224	298	326	90	208
Qir	169	252	208	252	77	160	255	76	210	367	426	442	269	295	157	280	237	0	284	240	356	299	183	381	147	304	98	243	324
Kharameh	84	248	83	330	197	107	210	194	271	122	243	245	178	459	128	404	106	284	0	419	165	203	352	286	258	61	363	40	86
Mohr	509	240	548	269	401	484	579	416	295	591	776	783	609	45	284	759	561	240	419	0	696	739	180	494	487	642	167	388	451
Safashahr	187	347	148	565	380	317	412	280	345	379	107	434	287	651	250	437	347	356	165	696	0	42	518	292	351	103	475	206	78
Bavanat	230	290	191	608	423	360	455	223	288	422	460	467	293	694	288	408	160	299	203	739	42	0	555	404	294	228	513	243	117
Gerash	359	500	413	23	185	247	189	245	522	286	573	597	468	146	318	283	314	183	352	180	518	555	0	530	318	414	90	312	473
Rostam	180	79	223	507	358	123	426	283	17	390	240	288	135	515	232	620	348	381	286	494	299	404	530	0	318	314	457	255	288
Farashband	164	105	177	356	231	294	389	71	305	356	421	438	264	442	124	414	224	147	258	487	351	294	318	318	0	299	260	227	290
Arsenjan	135	295	96	513	328	165	360	228	293	327	210	274	235	599	201	385	298	304	61	642	103	228	414	314	299	0	426	101	43
Khonj	286	418	332	113	169	258	220	169	441	317	491	555	387	133	237	373	326	98	363	167	475	513	90	457	260	426	0	322	403
Sarvestan	83	217	130	289	156	65	169	163	240	133	283	285	185	427	97	363	90	243	40	388	206	243	312	255	227	101	322	0	143
Saadatshahr	119	250	66	450	101	210	313	226	272	207	157	158	196	490	175	482	208	324	86	451	78	117	473	288	290	43	403	143	0

Table 2 – The centroid of demand for products in Fars healthcare supply networ

Customer	1									
Time period	1	2	3	4	5	6	7	8	9	10
Products	Centroid of Demand									
LARONIDASE 100IU/ML 5ML VIAL	2.45	2.22	1.95	2.29	2.26	2.15	1.87	2.01	2.52	2.29
ANTIHEMOPHILIC FACTOR XIII 250U VIAL	10.30	10.26	7.88	9.78	9.16	10.08	10.32	8.44	9.48	8.43
ERYTHROPOIETIN 10000IU/0.5 ML SYRINGE	94.66	93.78	107.84	87.02	115.17	112.09	84.60	86.96	115.47	87.22
ACITRETIN 25MG CAP	885.14	857.19	950.49	813.15	1062.74	1095.03	914.84	840.24	1097.50	934.97
LEVETIRACETAM 500 MG TAB	3823.83	4019.05	3098.07	3226.06	3796.54	3067.64	3557.95	3083.96	3094.24	3059.44
CO-AMOXICLAV 228 (200/28.5)/5ML POW SUSP	1164.79	1014.08	1127.34	880.01	1054.63	946.78	854.54	1032.16	960.60	855.02
GRANISETRON 3MG/3ML AMP	912.49	780.44	952.49	819.65	826.25	849.38	823.92	951.34	867.73	794.06
RIVASTIGMINE 1.5MG CAP	8126.18	7083.54	7734.49	8077.41	9647.96	7102.95	9069.00	9690.79	7793.43	7798.10
LAMOTRIGINE 100MG TAB	24203.46	20745.61	23794.18	20075.89	23630.94	21955.82	25758.05	26793.99	22046.30	20337.54
POTASSIUM CHLORIDE 15% 50ML VIAL	1136.41	1495.93	1269.34	1356.84	1212.52	1102.93	1314.06	1314.76	1460.97	1251.78
CITICOLINE SODIUM 250MG/2ML AMP	2857.29	2099.95	2153.59	2122.04	2910.06	2546.92	2538.41	2305.96	2114.15	2155.04
POVIDONE IODINE 7.5% 1L SCRUB	137.65	155.45	135.85	135.14	152.94	145.28	155.16	176.78	181.58	161.75
SOMATROPIN 10MG 1.5ML PEN	11.35	9.89	13.04	10.03	9.87	10.43	11.18	10.15	12.79	11.27
ARTIFICIAL TEARS 10 ML OPH DROP	3255.00	3496.55	2954.48	3051.46	3548.21	3476.97	3396.08	2873.97	3695.36	2736.18
KETOROLAC 30MG/ML INJ	2843.50	3110.71	2696.29	3645.46	2988.26	3172.66	2671.90	3230.70	3650.71	3311.79
METRONIDAZOLE 500MG/100ML VIAL P-BOTTLE	2224.33	2135.69	1947.52	1896.43	2546.84	2618.58	2112.29	2197.04	1930.21	2472.39
FLUOROMETHOLONE 0.1% 5ML OPH DROP	3382.99	3398.18	3653.02	3212.13	3019.55	2941.16	3511.50	3702.58	3312.60	3050.12
SALBUTAMOL SULFATE 2MG/5ML 120ML SYRUP	2963.96	3008.89	2943.28	3451.57	2925.33	2798.63	2949.09	3172.62	2922.59	3656.51
CHLORAMPHENICOL 0.5% OPH DROP	3318.29	3299.71	4220.42	3197.47	4241.77	3586.20	3369.02	3904.57	3292.53	3362.92
SILVER SULFADIAZINE 10MG/G 50G CREAM	1602.99	1198.71	1226.79	1242.60	1287.61	1429.73	1212.97	1340.34	1412.50	1336.17
CLOZAPINE 100MG TAB	10869.38	12963.60	9870.46	12621.26	9495.42	11154.12	10470.59	9855.29	10445.84	9779.54
CEFIXIME 400MG CAP	6224.07	5016.79	5826.48	5854.09	5696.92	5870.07	4948.87	5415.91	5656.08	5889.86
CHLORPROMAZINE HCL 100MG TAB	12305.34	11140.69	9383.75	10289.03	12021.00	9203.77	10484.70	9577.77	12094.70	9275.23
ROMIPLOSTIM 250MCG VIAL	1.64	1.65	1.43	1.26	1.41	1.44	1.34	1.55	1.42	1.30
METOCLOPRAMIDE 4MG/ML 15ML ORAL DROP	3590.97	4044.98	3154.58	3504.62	3926.14	3610.60	3959.91	3000.83	3113.67	3956.61
MULTIVITAMIN EFF TAB	19816.94	15672.36	16043.81	19937.90	16711.19	16982.90	19840.54	17173.82	16096.78	19345.16
INSULIN BIPHASIC ISOPHANE (70+30)U/ML 10ML VIAL	363.61	341.54	380.71	369.43	300.16	298.78	295.15	349.35	368.69	324.36
GANIRELIX 0.25MG INJ	28.20	29.86	29.15	28.67	30.14	27.97	25.02	29.11	28.03	26.78
PAROXETIN 20MG TAB	7782.23	7154.42	6615.23	6643.74	6370.51	8131.62	6227.75	8034.46	6255.68	6433.27
TACROLIMUS 0.1% 30G OINT	57.62	63.90	57.79	57.33	50.80	63.69	55.47	68.30	55.64	49.90
INTERFERON B 1A 30 MCG AMP	35.04	33.11	36.28	35.68	41.76	37.57	42.10	38.59	36.68	40.07
CISPLATIN 50MG VIAL	95.52	105.96	106.59	98.93	129.26	124.86	100.85	101.83	100.82	96.32

Table 3 – Products classification

Index	Product class	Index	Product class	Index	Product class
1	Analgesic drugs	18	Blood products	34	Anesthetics
2	Anthelmintics	19	Bone modulating	35	Muscle relaxants
3	Antibacterials	20	Anti-asthma	36	Neuromuscular blockers
4	Antidepressants	21	Cardiovascular drugs	37	Parasympathomimetics
5	Anti-diabetics	22	Antidote and antagonists	38	Pesticides and repellents
6	Antiepileptics	23	Contrast media	39	Prostaglandins
7	Antifungals	24	Corticosteroids	40	Sex hormones
8	Antigout drugs	25	Cough suppressants	41	Suspending agents
9	Anti-histamines	26	Dermatological	42	Stimulants and anorectics
10	Antimalarials	27	Disinfectants	43	Thyroid drugs
11	Antimigraine drugs	28	Dopaminergics	44	Vaccines
12	Antimuscarinics	29	Electrolytes	45	Herbal drugs
13	Antineoplastics	30	Gastrointestinal drugs	46	Others
15	Antiprotozoals	31	Anesthetics	47	Nutritional agents and vitamins
16	Antivirals	32	Hypothalamic and pituitary		
17	Sedatives & hypnotics	33	Immunosuppressants		

developed by Deb et al. based on the genetic algorithm [53]. Like other evolutionary algorithms, in the first step NSGA-II generates random solutions with the population of μ. In addition, each solution is evaluated by fitness functions, and, based on this evaluation, Pareto fronts are created by non-domination sorting. In the next step, each solution receives a rank equal to the level of the front that it belongs to. Then the crowding distance between the solutions on each front is measured. The selection procedure is the binary tournament method. The winner is the solution with the higher rank, and if the ranks are equal, the winner is the one with the higher crowding distance. The rest of the NSGA-II procedure is exactly the same as the genetic algorithm [54]. Moore and Chapman were the first to present MOPSO [55]. The procedure of MOPSO is similar to PSO. The only difference is that since the problem is multi-objective, instead of determining global best solution (G-best), the Pareto front would be determined. So, an archive including all of non-dominated solutions found in each iteration are stored. The steps of MOPSO are:

1) Initialize random solutions with the population of μ and the archive of non-dominated solutions.
2) For each solution: a) Select the G-best from the archive; b) Update velocity; c) Update position
3) Update the archive of non-dominated solutions
4) Repeat [55].

In the presented case study, to measure TRCE, a vector with B=1,000,000 array for each probabilistic and fuzzy numbers based on their probability density function or fuzzy membership function is generated by MATLAB 2012a. Then the histogram and Kolmogorov-Smirnov test is calculated to estimate the possibility distribution function of TRCE.

5.2 Results

The presented problem is solved by NSGA-II, MOPSO, and M-NRGA. The input parameters of these algorithms are given in *Table 4*. Four common measures are used to compare the algorithms. The most important index is the quality of solutions. This index cannot be measured for a Pareto front individually and must be calculated comparing to another Pareto front. Assume P_i is the Pareto front resulted by algorithm *i,* and P_j is the Pareto front resulted by algorithm *j,* then the quality index for algorithm *i* and *j* ($Q(P_i, P_j)$) can be calculated by *Equations 29* and *30*.

Table 4 – The input parameters of NSGA-II, MOPSO and M-NRGA

NSGA-II	Number of population	Maximum iteration	Crossover rate			Mutation%
	100	100	0.65			5
MOPSO	Number of population	Maximum iteration	C_1	C_2	ω	Mutation%
	100	100	1.9	2.1	0.8	5
M-NRGA	Number of population	Maximum iteration	P_e		P_t	Mutation%
	100	100	Adjustable			5

$$C(P_i,P_j)=\frac{\text{Number of solutions in } P_j \text{ dominated by solutions in } P_i}{\text{Number of solutions in } P_j} \quad (29)$$

$$Q(P_i,P_j)=\frac{C(P_i,P_j)}{C(P_i,P_j)+C(P_j,P_i)} \quad (30)$$

Considering *Equations 29* and *30*, it is clear that $Q(P_i, P_j)+Q(P_j, P_i)=1$. For the quality index, if $Q(P_i, P_j)>Q(P_j, P_i)$, then the Pareto front resulted by algorithm i is better than the Pareto front resulted by algorithm j [56].

The next index for evaluating the performance of a multi-objective algorithm is the diversity of the solutions in the Pareto front ($D(P_i)$). The higher value of this index shows the better performance of the multi-objective algorithm. The diversity of solutions in a Pareto front is calculated as presented in *Equation 31*.

$$D(P_i)=\sum_{z=1}^{j}\max_{k,l}\{|Z_j(X_k)-Z_j(X_l)|\} \quad (31)$$

where Z_j is the objective function j and X_k is the solution in Pareto front P_i [56]. Two other indexes are CPU time and the number of solutions in the Pareto front (NSPF). The higher number of solutions in the Pareto front is more preferable because it can give the decision makers more options. We solve the presented case study 100 times. For the presented problem, *Table 5* shows the quality index for presented algorithms, and other indexes are presented in *Table 6*.

As presented in *Table 5*, the average of Q(MOPSO,NSGA-II) is higher than Q(NSGA-II,MOPSO), so, based on the quality index, the first assumption is that MOPSO performs better than NSGA-II. Similarly, based on the quality index, we can assume that M-NRGA performs better than both MOPSO and NSGA-II. *Table 6* shows that, on average, NSGA-II has better performance in CPU time. In addition, the average number of solutions in the Pareto front is higher in M-NRGA. The average diversity of the solutions in the Pareto front is higher in M-NRGA. It should be mentioned, since in the proposed M-NRGA P_e present of solutions are selected based on elitism from the elitist solutions in the first front, by adjusting P_e the number of solutions in the Pareto front can be adjusted to be at least equal to a fix number. In this paper, we consider 30 as the minimum number of solutions in the Pareto front.

To ensure that the presented algorithm can solve the network design problem efficiently and in reasonable time, statistical tests are implemented [57]. The confidence level of 99% is considered for all of the tests. The first test is if NSGA-II performs better than the proposed M-NRGA in each index, and the second one is if MOPSO performs better than M-NRGA in each index at the confidence level of 99%. As presented in *Table 7*, both MOPSO and NSGA-II have a better CPU time comparing to M-NRGA. However, in terms of the

Table 5 – Quality index for presented algorithms

Sample size	$Q(P_i,P_j)$	Mean			Standard deviation		
		NSGA-II	MOPSO	M-NRGA	NSGA-II	MOPSO	M-NRGA
100	NSGA-II	-	0.4877	0.3563	-	0.12	0.09
100	MOPSO	0.5123	-	0.3649		-	0.08
100	M-NRGA	0.6437	0.6351	-	0.21	0.18	-

Table 6 – The value of indexes for presented algorithms

	Mean				Standard deviation		
Index	Sample size	NSGA-II	MOPSO	M-NRGA	NSGA-II	MOPSO	M-NRGA
CPU Time [s]	100	7,439.34	8,643.21	8,941.62	632.71	501.51	781.42
NSPF	100	18.42	16.23	30	4.32	3.21	0
	100	5,294,031.11	7,768,633.35	8,345,223.32	123,122.74	143,287.46	168,231.51

Table 7 – The statistical tests results for all hypotheses

H_0 (null hypothesis)	Test problem index	P-value
NSGA-II performs better than M-NRGA	Quality index of the Pareto front	0.000
	CPU time [s]	1.000
	Number of solutions in the Pareto front	0.000
	Diversity of the Pareto front	0.000
MOPSO performs better than M-NRGA	Quality index of the Pareto front	0.000
	CPU time [s]	0.342
	Number of solutions in the Pareto front	0.000
	Diversity of the Pareto front	0.000

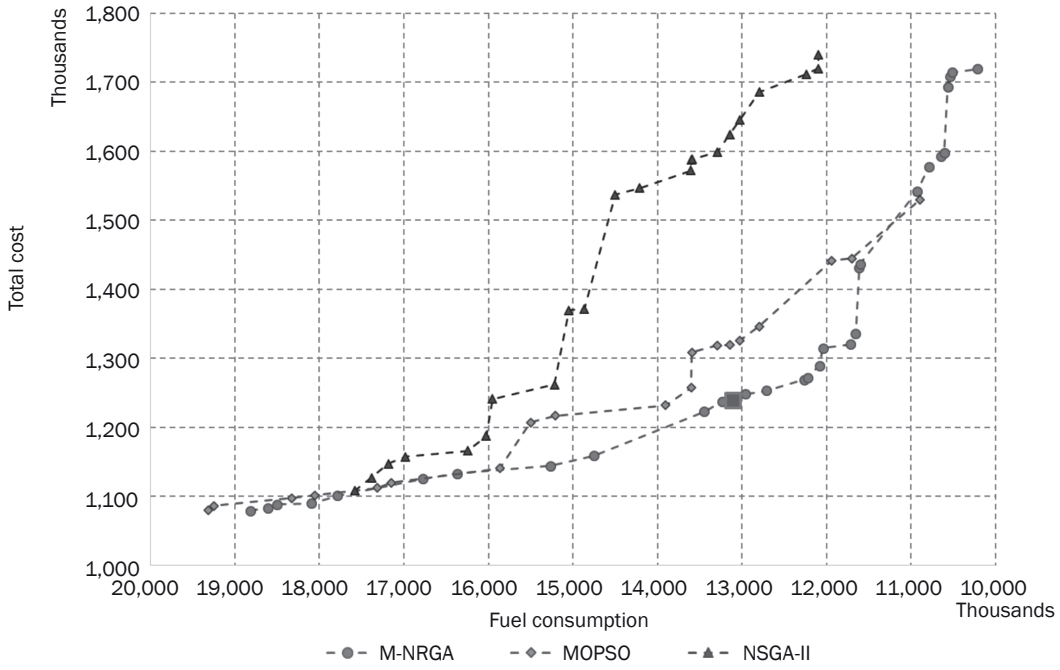

Figure 5 – The best Pareto fronts for the Fars healthcare supply network design problem, based on quality index

quality index of the Pareto front, number of solutions in the Pareto front, and Pareto front diversity, the performance of M-NRGA is better.

As mentioned before, the most important index for evaluating Pareto fronts is the quality index. The best Pareto fronts for the Fars healthcare supply network design problem, based on this index, are illustrated in *Figure 5* and *Table 8*. As presented in *Table 8*, according to *Equation 18*, the diversity of the solutions in the Pareto front resulted from M-NRGA amounts to 9,235,474.32, from MOPSO to 8,868,654.35, and from NSGA-II to 6,119,401.00.

Based on *Equations 29* and *30*, Q(M-NRGA,NSGA-II)=1 and Q(M-NRGA,MOPSO)=0.966. So, according to these indexes, M-NRGA performs better than the other two algorithms. However, in the CPU time index, NSGA-II preforms better.

To find the best solution in the Pareto front resulted from M-NRGA, as presented in the solution algorithm, PROMETHEE-II was applied. The best solution is also shown in *Figure 7*. For this solution, *Objective function 2* – minimizing total cost – is: 1,237,447.6 $, and *Objective function 3* – minimizing fuel consumption – is: 13,233,837.6 liters.

Table 8 – Best Pareto front for the presented problem based on quality index

Algorithm	Z_1	Z_2	CPU time [s]	NSPF	$D(P_i)$
M-NRGA	1,079,481.97	10,217,546.41	8,746.21	30	9,235,474.32
MOPSO	1,079,562.97	10,894,725	8,668.34	19	8,868,573.35
NSGA-II	1,107,998	12,094,725	7,365.41	22	6,119,401.00

Table 9 – Descriptive statistics of TRCE

			Statistic	Std. error
TRCE	Mean		32,007,127,597.94434	8,261,135.309457544
	95% confidence Interval for mean	Lower bound	31,990,936,055.797	
		Upper bound	32,023,319,140.09168	
	5% Trimmed mean		32,005,466,357.367813	
	Median		31,998,456,877.6218	
	Variance		6.8246288E+19	
	Std. deviation		8,261,131,178.888857	
	Minimum		-9,849,490,945.33062	
	Maximum		7.33051201511E+10	

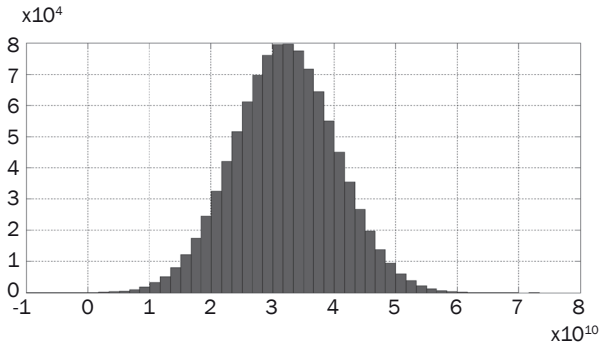

Figure 6 – Histogram of TRCE for Fars healthcare supply network

TRCE vector is calculated by *Equation 27*. A vector with B=1,000,000 arrays for each probabilistic and fuzzy number based on their probability density function or fuzzy membership function is generated by MATLAB 2012a for measuring TRCE. *Table 9* shows the descriptive statistics of TRCE in the Fars healthcare supply network. The average of TRCE is: 32,007,127,597.94 grams, and the standard deviation of TRCE is: 8,261,131,178.88.

The histogram of TRCE is illustrated in *Figure 6*. According to this histogram, we expect that the probability distribution function of TRCE would be normal. The Kolmogorov-Smirnov test is applied to test the normality of TRCE. *Figure 7* presents the normal Q-Q plot of TRCE. It proves that the probability distribution function of TRCE is normal.

6. CONCLUSION AND FUTURE STUDY

In recent history, global warming has been one of the most important challenges for humanity. Understanding carbon footprint is vital in overcoming this challenge. In this paper, we provided a computational method for measuring TRCE in a healthcare supply network. In the first step, a mathematical model for designing a proper supply network under uncertainty was developed. To solve this model, we proposed a two-phase algorithm based on NRGA and the PROMETHEE-II method. The statistical tests showed that the proposed algorithm has better performance in solving the model in comparison to NSGA-II and MOPSO. In the proposed algorithm, the number of solutions in the Pareto front can be adjusted to be at least equal to a fixed number. This can provide more possibilities for decision-makers to obtain optimal solutions in real-world problems. In the next step, a computational method based on Monte Carlo was developed for measuring TRCE. The proposed approach was applied to the Fars healthcare supply network. After solving the model, the total cost is $1,237,447.6, and the fuel consumption is 13,233,837.6 liters in the planning time horizon. The probability distribution function of TRCE is normal with the mean of 32,007,127,597.94 grams and variance of 6.8246E+19. The obtained results confirm the efficiency of the proposed approach as a practical tool for measuring TRCE. In this research, time windows for product delivery to distribution centers and

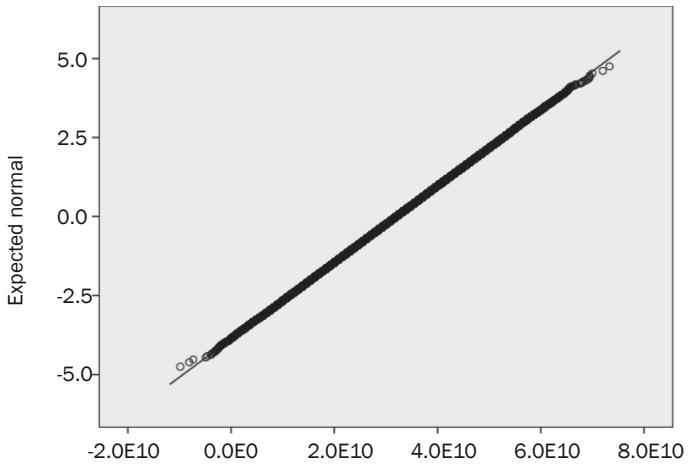

Test of normality			
	Kolmogorov-Smirnov[a]		
	Statistic	df	Sig.
TREC	0.001	999999	0.200*

* A lower bound of true significance
[a] Lilliefors significance correction

Figure 7 – Normal Q-Q plot of TRCE for Fars healthcare supply network

customers are not considered. Due to the importance of time windows in pharmaceutical substance delivery, further study is still required on this topic.

ACKNOWLEDGMENTS

We would like to express our appreciation to the Iran National Science Foundation (INSF) for the financial support of this study.

یثم نصرالهی دانشجوی دکتری[1]
E-mail: m_nasrollahi@ut.ac.i
روفسور دکتر **جعفر رزمی**[1]
E-mail: jrazmi@ut.ac.i
روفسور دکتر **رضا قدسی**[1]
E-mail: ghodsi@ut.ac.i
ایران، تهران، خیابان کارگر شمالی، پردیس دانشکده‌های فنی دانشگاه تهران، انشکده مهندسی صنایع

یک روش محاسباتی برای اندازه‌گیری میزان انتشار کربن ناشی از حمل و نقل در زنجیره‌تأمین سلامت و درمان در شرایط عدم قطعیت مختلط: یک مطالعه تجربی

یکیده:
کی از اقدامات اساسی برای مقابله با گرمایش جهانی اندازه‌گیری میزان انتشار ربن است. این پژوهش به ارایه یک روش محاسباتی برای اندازه‌گیری میزان نتشار کربن ناشی از حمل و نقل در زنجیره‌تأمین سلامت و درمان پرداخته است. ز آنجاکه ساختار شبکه نقش موثری در میزان انتشار کربن دارد، در ابتدا یک دل برنامه‌ریزی ریاضی برای طراحی شبکه تأمین با ساختار مسیریابی – کانیابی دو گرافی تحت شرایط عدم قطعیت تقاضا و عدم قطعیت مصرف سوخت رایه گردید. توابع هدف نیز کمینه‌سازی هزینه کل و کمینه سازی مصرف سوخت رنظر گرفته شده‌اند. در این مدل کل تقاضای مشتریان در هر دوره زمانی باید اسخ داده شود و پس‌افت مجاز نیست. تعداد و ظرفیت وسایط نقلیه معین و غیر ممنوع است. همچنین میزان مصرف سوخت به فاصله طی شده، وسیله نقلیه، رایط جاده و میزان بار وسیله نقلیه وابسته است. برای مواجهه با عدم قطعیت قاضا از روش مرکز هندسی بهره گرفته شد. برای حل مدل نیز توسعه‌ای از لگوریتم NRGA ارایه گردید. در ادامه براساس روش مونت کارلو، روشی رای محاسبه میزان انتشار کربن ناشی از حمل و نقل در شبکه تأمین ارایه شد. ر نهایت، براساس مدل ارایه شده یک مطالعه موردی در کشور ایران - استان ارس انجام شد. نتایج حاصله نشان داد که مدل ارایه شده یک ابزار کاربردی ناسب برای طراحی شبکه تأمین سلامت و درمان و محاسبه میزان انتشار کربن اشی از حمل و نقل است.

لمات کلیدی: سلامت و درمان؛ اثر گلخانه‌ای؛ شبکه تأمین؛ انتشار کربن؛ مونت ارلو

REFERENCES

[1] Martens P. *Health and climate change: modelling the impacts of global warming and ozone depletion.* 1st ed. Routledge; 2014.

[2] Ali A, Amin SE, Ramadan HH, Tolba MF. Enhancement of OMI aerosol optical depth data assimilation using artificial neural network. *Neural Computing and Applications*. 2013;23(7-8): 2267-2279. Available from: https://doi.org/10.1007/s00521-012-1178-9

[3] Pachauri RK, Allen MR, Barros VR, Broome J, Cramer W, Christ R, et al. *Climate Change 2014: Synthesis Report.* Contribution of Working Groups I, II and III to the Fifth Assessment Report of the Intergovernmental Panel on Climate Change, 2014. Available from: https://www.ipcc.ch/report/ar5/syr

[4] Peters GP, Andrew RM, Boden T, Canadell JG, Ciais P, Le Quere C, et al. The challenge to keep global warming below 2 °C. *Nature Clim Change*. 2013;3(1): 4-6. Available from: http://dx.doi.org/10.1038/nclimate1783

[5] Reddy PP. Causes of Climate Change. In: *Climate Resilient Agriculture for Ensuring Food Security.* 1st ed. Springer; 2015. p. 17-26.

[6] Meinshausen M, Meinshausen N, Hare W, Raper SCB, Frieler K, Knutti R, et al. Greenhouse-gas emission targets for limiting global warming to 2°C. *Nature*. 2009;458(7242): 1158-1162. Available from: http://dx.doi.org/10.1038/nature08017

[7] Plambeck EL. Reducing greenhouse gas emissions through operations and supply chain management. *Energy Economics*. 2012;34(Suppl.1): 564-574. Available from: http://dx.doi.org/10.1016/j.eneco.2012.08.031

[8] IPCC. *Mitigation of climate change: Contribution of working group III to the fourth assessment report of the Intergovernmental Panel on Climate Change*. Intergovernmental Panel on Climate Change; 2007. 851 p.

[9] Mula J, Peidro D, Poler R. The effectiveness of a fuzzy mathematical programming approach for supply chain production planning with fuzzy demand. *International Journal of Production Economics.* 2010;128(1): 136-143. Available from: http://dx.doi.org/10.1016/j.ijpe.2010.06.007

[10] Selim H, Ozkarahan I. A supply chain distribution network design model: An interactive fuzzy goal programming-based solution approach. *International Journal of Advanced Manufacturing Technology.* 2008;36(3-4): 401-418. Available from: https://doi.org/10.1007/s00170-006-0842-6

[11] Acquaye A, Genovese A, Barrett J, Koh SCL. Benchmarking carbon emissions performance in supply chains. *Supply Chain Management: An International Journal*. 2014;19(3): 306-321. Available from: http://www.emeraldinsight.com/10.1108/SCM-11-2013-0419

[12] O'Shea SJ, Allen G, Fleming ZL, Bauguitte SJ-B, Percival CJ, Gallagher MW, et al. Area fluxes of carbon dioxide, methane, and carbon monoxide derived from airborne measurements around Greater London: A case study during summer 2012. *Journal of Geophysical Research: Atmospheres.* 2014;119(8): 4940-4952. Available from: http://doi.wiley.com/10.1002/2013JD021269

[13] Benjaafar S, Li Y, Daskin M. Carbon Footprint and the Management of Supply Chains: Insights From Simple Models. *IEEE Transactions on Automation Science and Engineering*. 2012;10(1): 99-116. Available from: https://ieeexplore.ieee.org/document/6248180

[14] Carling K, Han M, Håkansson J, Meng X, Rudholm N. Measuring transport related CO 2 emissions induced by online and brick-and-mortar retailing. *Transportation Research Part D.* 2015;40: 28-42. Available from: http://dx.doi.org/10.1016/j.trd.2015.07.010

[15] Minx JC, Wiedmann T, Wood R, Peters GP, Lenzen M, Owen A, et al. Input–output analysis and carbon footprinting: an overview of applications. *Economic Systems Research*. 2009;21(3): 187-216. Available from: https://doi.org/10.1080/09535310903541298

[16] Jaegler A, Burlat P. Carbon friendly supply chains: a simulation study of different scenarios. *Production Planning & Control*. 2012;23(4): 269-278. Available from: https://doi.org/10.1080/09537287.2011.627656

[17] Tian Y, Liu Q. The Study about the Calculation Method of Product Carbon Footprint during the Flow Manufacturing Process. *Journal of Low Carbon Economy*. 2014;3: 1-6. Available from: http://dx.doi.org/

10.12677/jlce.2014.31001

[18] Mogensen L, Kristensen T, Nguyen TLT, Knudsen MT, Hermansen JE. Method for calculating carbon footprint of cattle feeds–including contribution from soil carbon changes and use of cattle manure. *Journal of Cleaner Production*. 2014;73: 40-51. Available from: https://doi.org/10.1016/j.jclepro.2014.02.023

[19] Kaydani H, Najafzadeh M, Hajizadeh A. A new correlation for calculating carbon dioxide minimum miscibility pressure based on multi-gene genetic programming. *Journal of Natural Gas Science and Engineering.* 2014;21(1): 625-630. Available from: https://doi.org/10.1016/j.jngse.2014.09.013

[20] Ryu BY, Jung HJ, Bae SH. Development of a corrected average speed model for calculating carbon dioxide emissions per link unit on urban roads. *Transportation Research Part D: Transport and Environment.* 2015;34: 245-254. Available from: https://doi.org/10.1016/j.trd.2014.10.012

[21] Ortmeyer TH, Pillay P. Trends in transportation sector technology energy use and greenhouse gas emissions. *Proceedings of the IEEE.* 2001;89(12): 1837-1847. Available from: http://ieeexplore.ieee.org/stamp/stamp.jsp?tp=&arnumber=975921&isnumber=21066

[22] Morrow WR, Gallagher KS, Collantes G, Lee H. Analysis of policies to reduce oil consumption and greenhouse-gas emissions from the US transportation sector. *Energy Policy.* 2010;38(3): 1305-1320. Available from: https://doi.org/10.1016/j.enpol.2009.11.006

[23] Lotfi MM, Tavakkoli-Moghaddam R. A genetic algorithm using priority-based encoding with new operators for fixed charge transportation problems. *Applied Soft Computing.* 2013;13(5): 2711-2726. Available from: https://doi.org/10.1016/j.asoc.2012.11.016

[24] Babazadeh A, Langerudi MF, Afkar N, Shahandashti KF. Parameter Selection In Particle Swarm Optimization For Transportation Network Design Problem. *arXiv preprint arXiv:14127185*. 2014. Available from: http://arxiv.org/ftp/arxiv/papers/1412/1412.7185.pdf

[25] Jang Y-J, Jang S-Y, Chang B-M, Park J. A combined model of network design and production/distribution planning for a supply network. *Computers & Industrial Engineering.* 2002;43(1-2): 263-281. Available from: http://linkinghub.elsevier.com/retrieve/pii/S0360835202000748

[26] Pontrandolfo P, Okogbaa OG. Global manufacturing: A review and a framework for planning in a global corporation. *International Journal of Production Research*. 1999;37(1): 1-19. Available from: https://doi.org/10.1080/002075499191887

[27] Wong KF, Beasley JE. Vehicle routing using fixed delivery areas. *Omega*. 1984;12(6): 591-600. Available from: https://doi.org/10.1016/0305-0483(84)90062-8

[28] Norouzi N, Sadegh-Amalnick M, Alinaghiyan M. Evaluating of the particle swarm optimization in a periodic vehicle routing problem. *Measurement*. 2015;62: 162-169. Available from: https://doi.org/10.1016/j.measurement.2014.10.024

[29] Huang Z, Geng K. Local search for dynamic vehicle routing problem with time windows. In: *Instrumentation and Measurement, Sensor Network and Automation (IMSNA), 2013 2nd International Symposium on. IEEE;* 2013. p. 841-4.

[30] Baldacci R, Mingozzi A, Roberti R. Recent exact algorithms for solving the vehicle routing problem under capacity and time window constraints. *European Journal of Operational Research.* 2012;218(1): 1-6. Available from: http://dx.doi.org/10.1016/j.ejor.2011.07.037

[31] Nadizadeh A, Hosseini Nasab H, Nasab HH. Solving the dynamic capacitated location-routing problem with fuzzy demands by hybrid heuristic algorithm. *European Journal of Operational Research.* 2014;238(2): 458-470. Available from: http://linkinghub.elsevier.com/retrieve/pii/S037722171400321X

[32] Vahdani B, Shekari DVN, Mousavi SM. Multi-objective, multi-period location-routing model to distribute relief after earthquake by considering emergency roadway repair. *Neural Computing and Applications.* 2016;30(3): 835-854. Available from: https://doi.org/10.1007/s00521-016-2696-7

[33] Ewbank H, Wanke P, Hadi-Vencheh A. An unsupervised fuzzy clustering approach to the capacitated vehicle routing problem. *Neural Computing and Applications.* 2015; 857-867. Available from: http://link.springer.com/10.1007/s00521-015-1901-4

[34] Dalfard VM, Kaveh M, Nosratian NE. Two meta-heuristic algorithms for two-echelon location-routing problem with vehicle fleet capacity and maximum route length constraints. *-Neural Computing and Applications.* 2013;23(7-8): 2341–2349. Available from: ttps://doi.org/10.1007/s00521-012-1190-0

[35] Escobar JW, Linfati R, Baldoquin MG, Toth P. A Granular Variable Tabu Neighborhood Search for the capacitated location-routing problem. *Transportation Research Part B*: Methodological. 2014;67: 344-356. Available from: https://doi.org/10.1016/j.trb.2014.05.014

[36] Hemmelmayr VC. Sequential and parallel large neighborhood search algorithms for the periodic location routing problem. *European Journal of Operational Research.* 2015;243(1): 52-60. Available from: https://doi.org/10.1016/j.ejor.2014.11.024

[37] Wang F, Lai X, Shi N. A multi-objective optimization for green supply chain network design. *Decision Support Systems*. 2011;51(2): 262-269. Available from: http://dx.doi.org/10.1016/j.dss.2010.11.020

[38] Srivastava SK. Green supply chain management: a state of the art literature review. *International journal of management reviews*. 2007;9(1): 53-80. Available from: https://ieeexplore.ieee.org/document/6852800

[39] Rahimi M, Baboli A, Rekik Y. Multi-objective inventory routing problem: A stochastic model to consider profit, service level and green criteria. *Transportation Research Part E: Logistics and Transportation Review.* 2017;101: 59-83. Available from: http://dx.doi.org/10.1016/j.tre.2017.03.001

[40] Marcon E, Chaabane S, Sallez Y, Bonte T, Trentesaux D. Simulation Modelling Practice and Theory A multi-agent system based on reactive decision rules for solving the caregiver routing problem in home health care. *Simulation Modelling Practice and Theory*. 2017;74: 134-151. Available from: http://dx.doi.org/10.1016/j.simpat.2017.03.006

[41] Mańdziuk J, Świechowski M. UCT in Capacitated Vehicle Routing Problem with traffic jams. *Information Sciences.* 2017;406: 42-56. Available from: https://doi.org/10.1016/j.ins.2017.04.020

[42] Puga MS, Tancrez J. A heuristic algorithm for solving

large location – inventory problems with demand uncertainty. *European Journal of Operational Research*. 2017;259(2): 413-423. Available from: https://doi.org/10.1016/j.ejor.2016.10.037

[43] Dehghani E, Behfar nima, Jabalameli MS. Optimizing location, routing and inventory decisions in an integrated supply chain network under uncertainty. *Journal of Industrial and Systems Engineering.* 2016;9(4): 93-111. Available from: http://www.jise.ir/article_16501_0ccd46eae583b5bc10ca6437f66f71ae.pdf

[44] Nasrollahi M, Amiri AS, Razmi J, Nasrollahi H. Bullwhip Effect in Different Network Configuration. *Applied Mathematics in Engineering Management and Technology.* 2015;3(4): 261-267.

[45] Safaei M, Thoben KD. Measuring and evaluating of the network type impact on time uncertainty in the supply networks with three nodes. *Measurement: Journal of the International Measurement Confederation.* 2014;56: 121-127. Available from: http://dx.doi.org/10.1016/j.measurement.2014.06.010

[46] Rezvani S. Ranking generalized exponential trapezoidal fuzzy numbers based on variance. *Applied Mathematics and Computation.* 2015;262: 191-198. Available from: http://linkinghub.elsevier.com/retrieve/pii/S0096300315004889

[47] Mousavi SM, Alikar N, Niaki STA, Bahreininejad A. Two tuned multi-objective meta-heuristic algorithms for solving a fuzzy multi-state redundancy allocation problem under discount strategies. *Applied Mathematical Modelling*. 2015;39(22): 6968-6989. Available from: http://linkinghub.elsevier.com/retrieve/pii/S0307904X15001298

[48] Al Jadaan O, Rajamani L, Rao CR. Non-dominated ranked genetic algorithm for solving multi-objective optimization problems. *Journal of Theoretical and Applied Information Technology.* 2008; 113-118. Available from: www.jatit.org/volumes/research-papers/Vol5No5/15Vol5No5.pdf

[49] Mousavi SM, Sadeghi J, Niaki STA, Tavana M. A bi-objective inventory optimization model under inflation and discount using tuned Pareto-based algorithms: NSGA-II, NRGA, and MOPSO. *Applied Soft Computing Journal.* 2016;43: 57-72. Available from: http://dx.doi.org/10.1016/j.asoc.2016.02.014

[50] Kilic HS, Zaim S, Delen D. Selecting "The Best" ERP system for SMEs using a combination of ANP and PROMETHEE methods. *Expert Systems with Applications.* 2015;42(5): 2343-2352. Available from: http://linkinghub.elsevier.com/retrieve/pii/S0957417414006587

[51] Athawale VM, Chakraborty S. Facility Location Selection using PROMETHEE II Method. *International Conference on Industrial Engineering and Operations Management Dhaka. January 9-10;* 2010.

[52] amar.sci.org.ir [Internet]. Available from: https://amar.sci.org.ir/index_e.aspx

[53] Deb K, Pratap A, Agarwal S, Meyarivan T. A fast and elitist multiobjective genetic algorithm: NSGA-II. *IEEE Transactions on Evolutionary Computation.* 2002;6(2): 182-197. Available from: https://ieeexplore.ieee.org/document/996017.

[54] Pasandideh SHR, Niaki STA, Asadi K. Bi-objective optimization of a multi-product multi-period three-echelon supply chain problem under uncertain environments: NSGA-II and NRGA. *Information Sciences.* 2015;292: 57-74. Available from: http://dx.doi.org/10.1016/j.ins.2014.08.068

[55] Moore J, Chapman R. *Application of particle swarm to multiobjective optimization.* Department of Computer Science and Software Engineering Department, Auburn University. 1999; 1-4. Available from: http://goo.gl/NPkun

[56] Azadeh A, Ravanbakhsh M, Rezaei-Malek M, Sheikhalishahi M, Taheri-Moghaddam A. Unique NSGA-II and MOPSO Algorithms for Improved Dynamic CMS by Considering Human Factors. *Applied Mathematical Modelling*. 2017;48: 655-672. Available from: http://linkinghub.elsevier.com/retrieve/pii/S0307904X17301221

[57] Montgomery DC, Runger GC. *Applied statistics and probability for engineers. 6th ed.* NJ: Wiley; 2007.